

Prediction of Fracture of Steel Moment Connection by Cyclic Loading with Various Deformation Amplitude

K. Suita, Y. Manabe, K. Takatsuka
Kyoto University, Japan

T. Tanaka & T. Tsukada
Kobe University, Japan



SUMMARY

This paper presents a method to evaluate the deformation capacity of welded moment connections under cyclic loading with various deformation amplitudes. From results of loading tests conducted with constant deformation amplitudes, the relationships between the deformation amplitude and number of cycles until fracture and the crack propagation at welds are obtained quantitatively. Next, cyclic loading tests by two different amplitudes were conducted with various combinations of amplitudes and orders. Results suggest that the deformation capacity are affected not only by the amplitude, but also by the order. Miner's rule may not be suitable for the prediction of fracture, but the deformation capacity is predicted by crack-propagation curves obtained from constant amplitude tests. Finally, loading tests by random amplitudes simulating seismic demands by long-period ground motions are conducted and the validity of the prediction method was examined.

Keywords: steel structure, moment connection, deformation capacity, cyclic loading test, crack propagation

1. INTRODUCTION

Recent advancements in engineering seismology has enabled precise prediction of long-period ground motions produced by ocean-trench earthquake such as the Nankai trough earthquake in Japan. The characteristics of these ground motions are different from conventional strong motion records by near fault earthquakes such as El Centro 1940, Taft 1952 and so on. The predominant periods are longer by two seconds or more and the duration of motion can be as long as ten minutes. Therefore, the response of earlier highrise buildings against long-period ground motions is drawing attention (Suita, 2012). The 2011 Great East Japan Earthquake was a typical ocean-trench earthquake and many tall buildings in the Tokyo metropolitan area were strongly shaken (Kasai et al. 2012). For tall buildings constructed by steel, it is necessary to evaluate the deformation capacity of moment connections subjected to a very large number of cyclic deformation in the plastic range.

Failure of welded moment connections due to cyclic inelastic behavior is investigated using the concepts of low-cycle fatigue by Kuwamura and Takagi 2004, Stojadinovic 2003, Campbell et al. 2008 and many other researchers. Deformation capacity until failure of connection is usually estimated by the fatigue damage index of Miner's rule (Miner, 1945) as cumulative damage calculated from the numbers of cycles. However, Zhou et al. (2008) and Kadono et al. (2008) show that the fatigue damage index is affected by the order of loading amplitude when the tests are conducted by variable amplitudes. Namely, the deformation capacity by increasing amplitude loadings are smaller than that by decreasing amplitude loadings, but the effect of the order of variable amplitudes is not well understood in previous studies.

This paper presents a method to estimate deformation capacity of welded moment connections subjected to variable amplitude cyclic loadings considering the order of loading amplitudes. Iyama and Ricles (2009) present a methodology using accumulated crack length. In this paper, in order to calculate fatigue damage, the length of crack at the failure of welds were closely observed in the constant amplitude cyclic loading tests and the crack propagation is formulated as the function of

the number of cycles and the loading amplitude. The validity of the proposed formulation is verified by comparing with test results conducted by two different constant amplitudes loadings and random amplitude loadings which simulate the seismic response of a tall building subjected to long-period ground motions.

2. TEST METHOD

The test specimens prepared for the present study were beam-column subassemblages as shown in Fig. 2.1. The beam was a wide flange section (H-500x200x10x16) of SN490B steel and the column was a square tube (RHS-350x350x22) of BCR295 steel. The beam-to-column connection was the shop-welded through-diaphragm type. The beam flange was connected by a CJP groove weld to the diaphragm plate (22mm thick, SN490C) and the beam web was connected by fillet welds to the column face. Welding details with no weld access hole (Fig. 2.2) are adopted and the CJP weld was conducted as follows: gas metal arc welding (GMAW) with CO₂ shielding, YGW-11 (JIS) solid electrode with a diameter of 1.2 mm, stringer beads, 4 layers and 5 passes, heat input:11-30kJ/mm and interpass temperature: 177-250°C. Tack welds for backing bars were avoided in the vicinity of the flange-web junction and beam flange sides. Backing bar is split into two pieces, and is placed from both sides of the beam web, and were left in place after welding. Ceramic weld tabs were used for run-off tabs and these tabs were removed after welding. These welding details are recommended in JASS 6 2007 as the most effective method to avoid premature fracture and widely used in Japan after the 1995 Kobe earthquake. Three rib stiffeners were placed at the vicinity of beam ends to prevent local buckling of the beam flange and web.

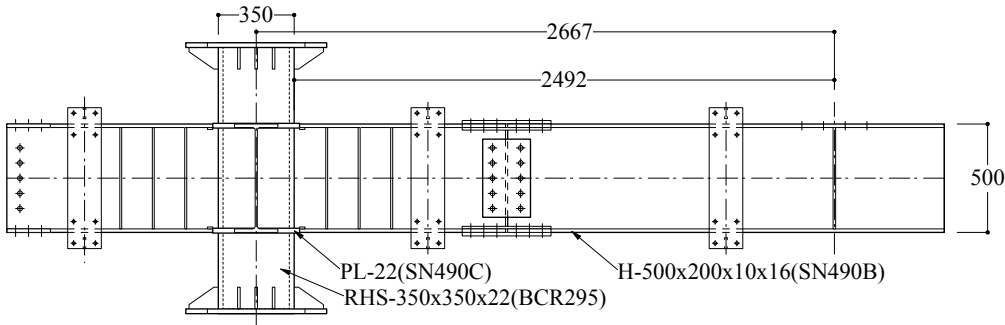


Figure 2.1. Dimensions of test specimen (unit:mm)

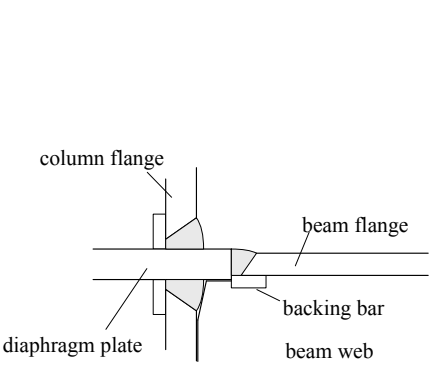


Figure 2.2 CJP welding Details

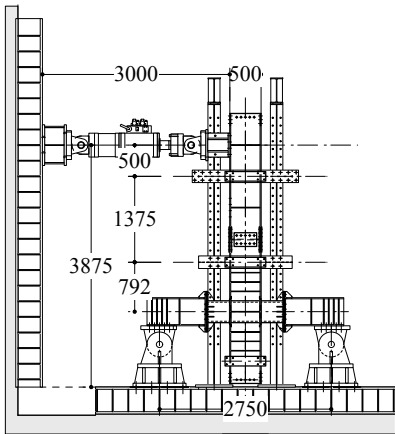


Figure 2.3 Load setup (unit:mm)

The test specimen was placed in the loading setup as shown in Fig. 2.3. The column ends were connected to column stubs, which were fastened to pin supports. The beam end was clamped to a dynamic actuator at a distance of 2.667m from the center line of the column. Two sets of lateral supports were placed on the beam to restrict out-of-plane deformation of the beam. The yield strength of beam flange and web obtained from coupon tests were 351MPa and 386MPa respectively, and the full plastic moment of the beam is 740kN•m. The elastic rotation θ_p corresponding to the full plastic moment of the beam at the face of the column is 0.00753rad and this value is used as the reference value to evaluate deformation of the specimen by ductility ratio $\mu = \theta/\theta_p$, where θ is the beam rotation.

3. CONSTANT AMPLITUDE CYCLIC LOADING TEST

8 specimens of constant amplitude cyclic loading tests were conducted. The specified beam rotation amplitudes were $1.2\theta_p$, $2\theta_p$, $3\theta_p$ and $4\theta_p$, and two tests were conducted for each amplitude. Figures 3.1 show example of moment versus rotation relationships obtained from tests. The failure of the specimen started by the crack initiated from the beam flange side of the bond of CJP weld at the start or end of the welding line after a number of cycles. The crack propagated gradually along the weld line increasing propagation rate and resulted in total fracture. The relationships between the ductility of loading amplitude μ and the number of cycles at fracture N_F are shown in Fig. 3.2 by a double logarithmic plot. The linear relationships in the plot is expressed by Eq. 3.1 from regression analysis.

$$N_F = 357\mu^{-2.44} \quad (3.1)$$

The propagation of cracks which lead to total fracture are shown in Fig. 3.3. The ordinate l is the length of a crack and the abscissa n is the number of cycles N normalized by N_F . From the observation of the curves in Fig. 3.3, it is found that the crack propagation behavior is divided in three stages, i.e. first: no crack observed, second: the cracks initiate and propagate gradually, third: the cracks propagate

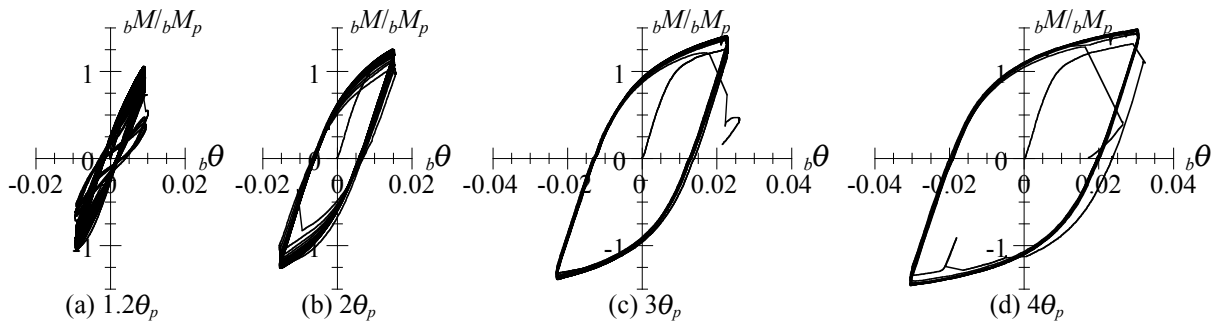


Figure 3.1 Example of moment versus rotation relationships by constant amplitude cyclic loading

Table 3.1 N_F and μ

μ	N_F
1.2	274
1.2	225
2.0	63
2.0	55
3.0	25
3.0	20
4.0	13
4.0	14

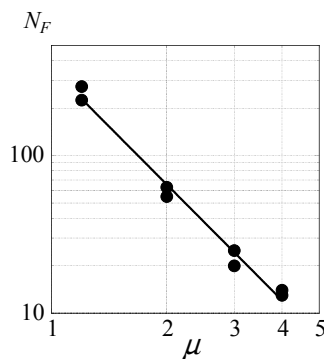


Figure 3.2 $N_F - \mu$ relationships

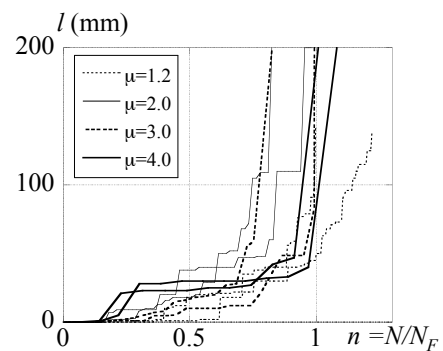


Figure 3.3 Crack propagation

rapidly to fracture. In order to evaluate damage to a welded connection, the crack propagation curve is formulated based on the relationships between the normalized number of cycles $n = N/N_F$ and crack propagation speed $v = dl/dN$ or its rate $a = d^2l/dN^2$ as shown in Fig. 3.4. In this concept, the normalized number of cycle n is regarded as the damage index. The relationships between damage index n and crack length l are formulated as follows.

$$\text{1st stage} \quad l = 0 \quad (0 \leq n \leq n_s) \quad (3.2)$$

$$\text{2nd stage} \quad l = a_1 N_F (n - n_s)^2 / 2 \quad (n_s \leq n \leq n_U) \quad (3.3)$$

$$\text{3rd stage} \quad l = v_2 (n - n_U) + l_U \quad (n_U \leq n) \quad (3.4)$$

where, n_s : n at the beginning of 2nd stage, n_U : n at the end of 2nd stage, l_U : length of crack at the end of 2nd stage, v_1 : crack propagation speed at the 2nd stage, a_1 : rate of v_1 , v_2 : crack propagation speed at the 3rd stage. The number of cycle at the beginning of the second stage is determined by visual observation during loading tests, and the beginning of the third stage is defined as the cycle just one cycle before the instance of total fracture. The coefficients n_s , l_U , a_1 and v_2 are determined from each test result and the relationships between the ductility with respect to loading amplitude μ and these coefficients are shown in Fig. 3.5. From regression analysis, the coefficients are obtained from the following relations. The beginning of the 2nd stage, n_s is defined as the mean value of test results, since it is considered as a constant value regardless of μ from Fig. 3.5(a).

$$n_s = 0.22 \quad (3.5)$$

$$l_U = -26.4\mu + 152 \quad (3.6)$$

$$a_1 = 5.37 (\mu - 1) \quad (3.7)$$

$$v_2 = 11353 \mu^{-1.23} \quad (3.8)$$

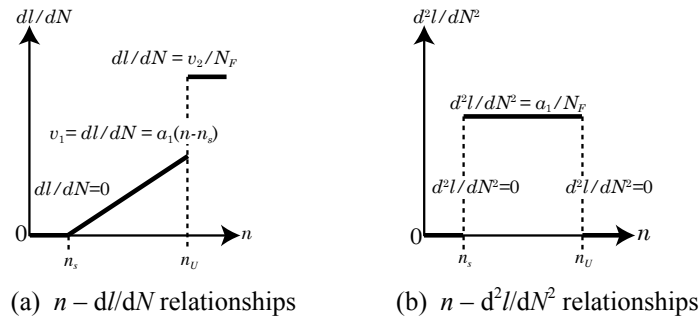


Figure 3.4 Concept of crack propagation formulation

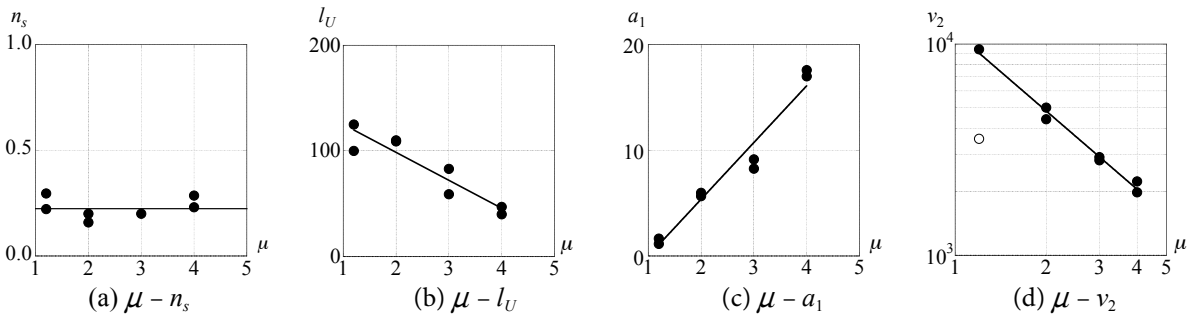


Figure 3.5 Relationships between μ and coefficients of crack propagation formulation

4. TWO-STAGE CONSTANT AMPLITUDE TEST

4.1 Test results

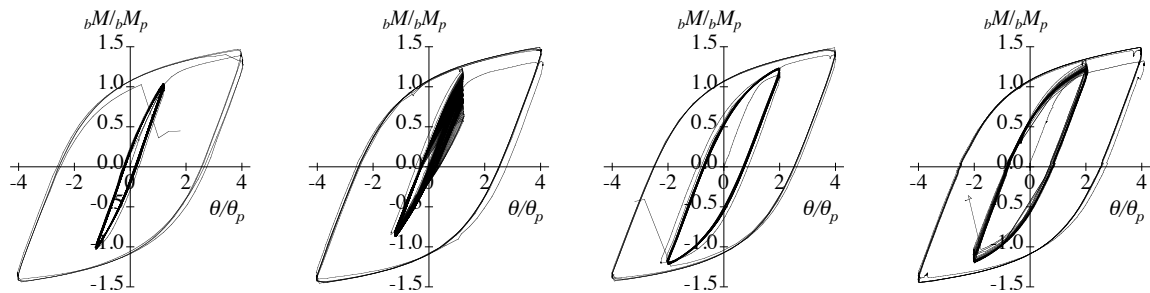
In order to investigate the effect of variable amplitude on cyclic loading behavior, two-stage constant

amplitude cyclic loading tests were conducted as the simplest loading protocol. In this test, the loading protocol consists of two different constant amplitude loadings. The ductility of the first and the second stage are μ_1 and μ_2 , the number of cycles are N_1 and N_2 , respectively. The damage index of the first stage d_1 is defined as N_1/N_{F1} , where N_{F1} is the number of cycles at the point of fracture calculated by Eqn. 3.1 with respect to ductility μ_1 . The tests are named as ' $\mu_1-d_1-\mu_2$ ', and the name of tests by same loading protocol are postfixed A or B. All tests by two-stage constant amplitude cyclic loadings are summarized in Table 4.1. The experimental value of damage index at the instance of fracture D_{exp} is defined by Eqn. 4.1, where N_i is the number of loaded cycles and the N_{Fi} is the number of cycles at fracture calculated by Eqn. 3.1 with respect to ductility amplitude μ_i .

$$D_{exp} = \sum_i \frac{N_i}{N_{Fi}} \quad (4.1)$$

The test No.1,2 and No.3,4 were loaded by the combination of ductility amplitude 1.2 and 4.0, and the damage index of each stage was specified approximately 0.5. The test No. 5 and 6 were specified larger damage index at the first stage. The test No. 7 and 8 were loaded by the combination of ductility amplitude 2.0 and 4.0, and the damage index of each stage was specified approximately 0.5. The test No.9,10 and No.11,12 were also the combination of ductility amplitude 2.0 and 4.0, and the damage index by ductility amplitude 2.0 is specified to be larger. The tests No.1, 2, 5, 7, 9 and 10 were loaded by increasing amplitude order and the tests No.3, 4, 6, 8, 11 and 12 were loaded by decreasing amplitude order.

Examples of moment versus rotation relationships by two-stage constant amplitude tests are presented in Fig. 4.1. The damage index after tests are presented in Fig. 4.2. From these results, it is found that the damage index of the tests loaded by increasing amplitude order have small damage index less than 1.0 and the tests loaded by decreasing amplitude order have larger damage index in many tests. According to Miner rule, the damage index D_{exp} should be 1.0 for all tests. However, these test results



(a) No.1(1.2–0.47–4.0A) (b) No.3 (4.0–0.58–1.2A) (c) No.7 (2.0–0.43–4.0) (d) No.8 (4.0–0.58–2.0)

Figure 4.1 Example of moment versus rotation relationships by two-stage constant amplitude tests

Table 4.1 Summary of two-stage constant amplitude test

No.	Test	μ_1	N_1	d_1	μ_2	N_2	D_{exp}
1	1.2–0.47–4.0A	1.2	108	0.47	4.0	5	0.79
2	1.2–0.47–4.0B					6	0.86
3	4.0–0.58–1.2A	4.0	7	0.58	1.2	173	1.34
4	4.0–0.58–1.2B					197	1.48
5	1.2–0.73–4.0	1.2	167	0.73	4.0	1	0.80
6	4.0–0.83–1.2	4.0	10	0.82	1.2	50	1.02
7	2.0–0.43–4.0	2.0	28	0.43	4.0	6	0.88
8	4.0–0.58–2.0	4.0	7	0.58	2.0	27	0.98
9	2.0–0.64–4.0A	2.0	42	0.64	4.0	4	0.92
10	2.0–0.64–4.0B					1	0.69
11	4.0–0.25–2.0A	4.0	3	0.25	2.0	61	1.19
12	4.0–0.25–2.0B					46	0.95

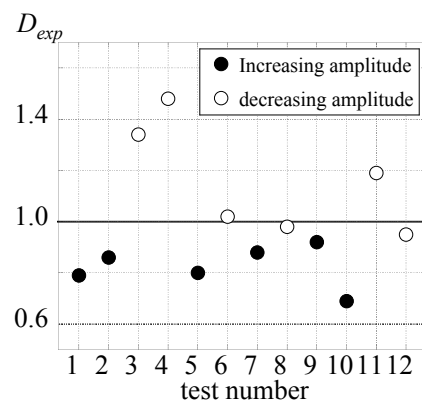


Figure 4.2 Damage index of two-stage constant amplitude tests

show that the deformation capacity of specimens loaded by variable amplitudes are affected by the order of amplitudes and this behavior is not evaluated by Miner's rule.

4.2 Damage index by crack propagation formulation

In order to evaluate the features revealed in tests, the present paper proposes a method to calculate the damage index from crack propagation curves. Fig. 4.3 shows the method to evaluate damage index at fracture. The crack length l is calculated by Eqn. 3.2–3.4. During the first stage of a loading test, the crack length is calculated by using the coefficients of Eqn. 3.5–3.8 associated with μ_1 . During the second stage, the coefficients of the equations are changed to the values associated with μ_2 and the calculation of the crack length is continued. When the calculated crack length reaches the length of the weld line, i.e. 200mm, the normalized number of cycles n is determined as the damage index D_{cal} . The results of D_{cal} obtained from these calculations are presented in Fig. 4.4. From the comparison between D_{exp} and D_{cal} , it is found that the proposed method using the crack propagation formulation is more effective than Miner's rule to evaluate damage index of specimens loaded by variable amplitudes.

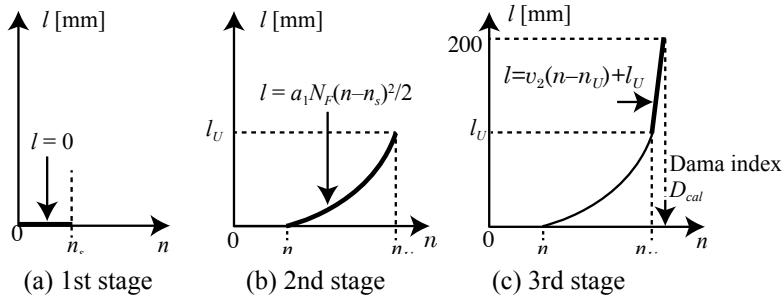


Figure 4.3 Crack propagation curves of two-stage constant amplitude test

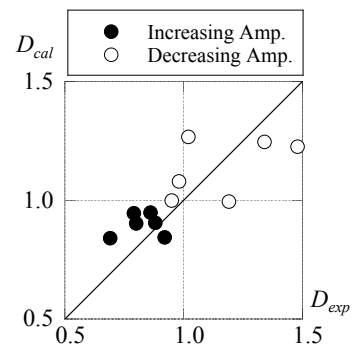


Figure 4.4 Damage index

5. RANDOM AMPLITUDE LOADING TEST

5.1 Loading protocol simulating seismic response of long-period ground motion

A loading protocol with random amplitude was developed based on simulated response of moment connections in highrise buildings subjected to long-period ground motions. A total of 89, synthetic long-period ground motions produced by three research groups, i.e. Kamae et al. (2004), Tsuruki et al. (2005), and Suzuki et. al. (2005) are used for the dynamic response analysis. The properties of the motions are shown in Table 5.1, and the velocity response spectra of representative motions are shown in Fig. 5.1. Two models representing early highrise buildings, height of 75m and 150m, are prepared for dynamic response analysis as shown in Fig. 5.2. These models are designed according to the

Table 5.1 Predicted long-period ground motion

Earthquake Researcher	Number of motion	Duration [s]	PGA [m/s ²]	PGV [m/s]
Tonankai by Suzuki	64	100–450	16–674	2–64
Tonankai by Tsuruki	23	300	70–216	7–63
Nankai by Kamae	2	290–440	68–674	–

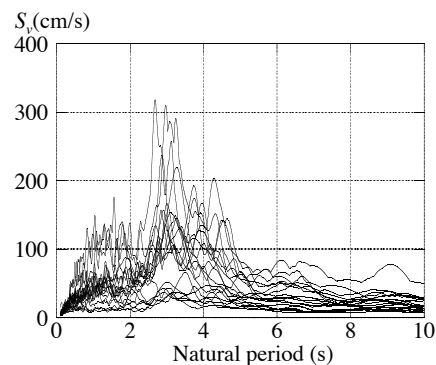


Figure 5.1 Example of velocity response spectrum of predicted Tonankai Earthquake

seismic regulations in the 1970s. The fundamental natural periods are 2.34s and 4.58s respectively. In earlier highrise design, plastic deformation of structural members, i.e. beams or braces, were permitted. The energy dissipation mechanism is expected to be quite different between earlier highrises and current highrises that employ dampers to control drift. From analysis results, four time histories of beam rotation were chosen for loading protocols as shown in Fig. 5.3. The locations of beam members with respect to chosen responses are indicated in Fig. 5.2 by black circles and names R1 – R4. Each response has the following characteristics. The R1 repeats many times with ductility amplitudes about 2. The R2 has many small amplitudes and only a few cycles with the amplitudes more than ductility 2. The R3 has many large cycles with ductility amplitudes near 4. The R4 repeats combinations of large ductility amplitude about 3 and many small amplitudes and has long duration.

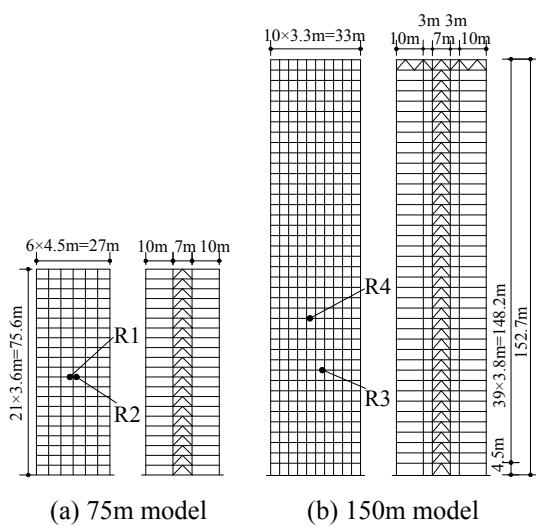


Figure 5.2 Analysis model

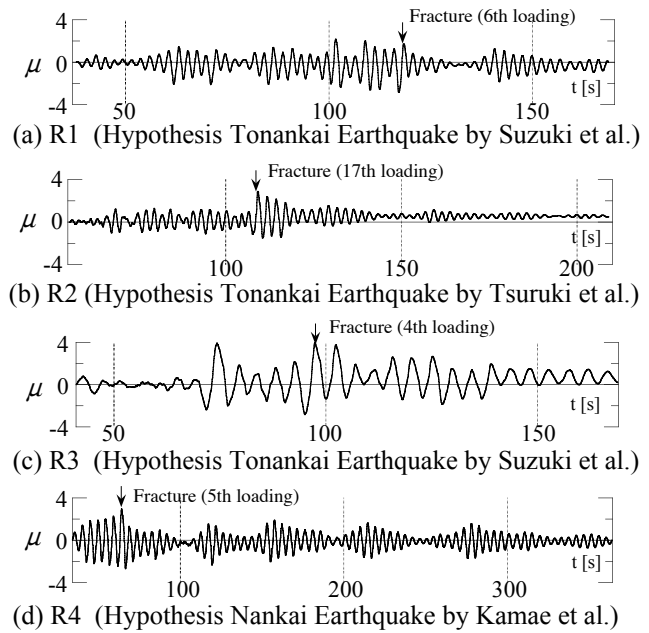


Figure 5.3 Time history of beam rotation for random loading

5.2 Random amplitude loading test

The moment versus rotation relationships obtained from random amplitude loading tests are shown in Fig. 5.4. The loadings were repeated until fracture of beam flange welds occurred. The instant of fracture is indicated in Fig. 5.3 with the number of repetition of loadings. From test results, since the minimum number of repetition of loading is 4 at R3, which has maximum ductility amplitudes 4, it is exhibited that the specimens, which is designed and fabricated in accordance with the current recommended practice, have sufficient deformation capacity against long period ground motions by hypothesized Nankai Trough earthquakes.

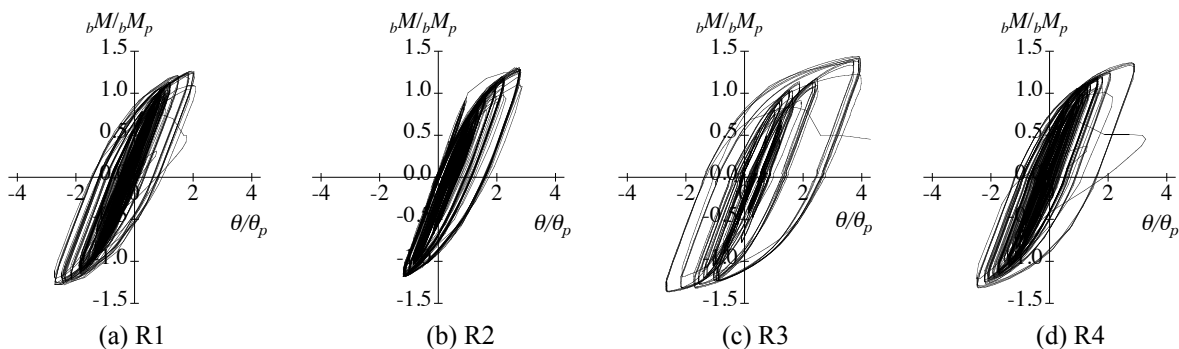


Figure 5.4 Moment versus rotation relationships by random amplitude cyclic loading test

In order to evaluate damage indices from the random amplitude tests, the time history of plastic components of the beam rotation is extracted from each test result. An example of time history of ductility is shown in Fig. 5.5. From this time history, the ductility amplitude and the number of excursions that cause damage to the connection were counted by rain-flow method (ASTM, 2005). As an example, Fig. 5.6 presents the sequence of excursion extracted from the time history of Fig. 5.5. The proposed method using crack propagation formulations were applied to the test results of random amplitude tests. The length of the crack is calculated by Eqns. 3.2–3.4, using the coefficients calculated by Eqns. 3.5–3.8 and the ductility of each excursion of the test result. In this calculation, the excursions those ductility are larger than 1.0 are taken to evaluate crack length. When the calculated crack length reaches the length of the weld line, 200mm, the normalized number of cycles n is determined as the damage index D_{cal} . An example of the result of test R1 is shown in Fig. 5.7. In the figure, the columns indicate ductility of excursions, as does Fig. 5.5, and the line indicates crack propagation. In case of test R1, fracture of the flange occurred during the 6th loading, but the crack propagation curve indicates that calculated instant of fracture is during the 9th loading. The cause of underestimation of damage is that the influence of loadings by small amplitudes are neglected. The crack propagation formulation is derived from constant amplitude tests that only include amplitudes larger than 1.0. However, the random amplitude loading test suggests that cycles whose amplitudes are smaller than 1.0 influence crack propagation.

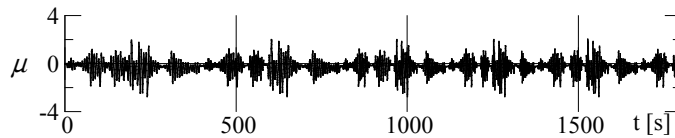


Figure 5.5 Example of time history of ductility in beam rotation (R1)

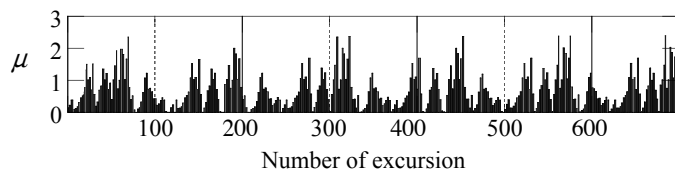


Figure 5.6 Example of sequence of extracted excursions and ductility (R1)

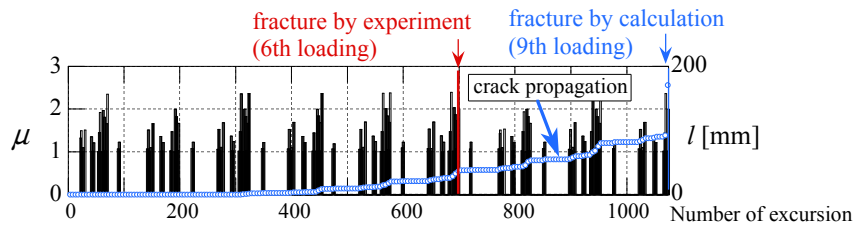


Figure 5.7 Damage evaluation by crack propagation (test R1, $\mu_0=1.0$)

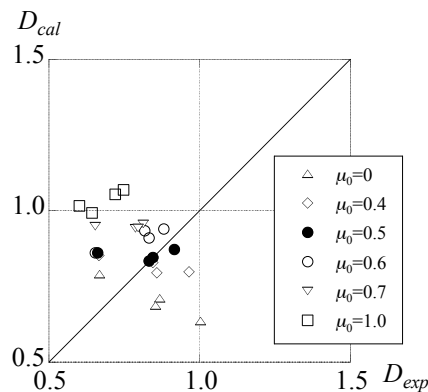


Figure 5.8 Effect of μ_0 on evaluation of damage index

In order to evaluate the effect of loadings by small amplitude, the minimum ductility of amplitude μ_0 , which is the minimum value of ductility taken into account, is varied between 0 to 1.0. The comparison of damage index between experimental value D_{exp} and calculated value D_{cal} are shown in Fig. 5.8. This figure shows that the differences between experimental values and calculated values become minimum when μ_0 is 0.5. From these investigations, the most adequate value of μ_0 was determined as 0.5 for the present tests. The results of evaluation of crack propagation for all tests calculated by setting the value of μ_0 as 0.5 are shown in Fig. 5.9.

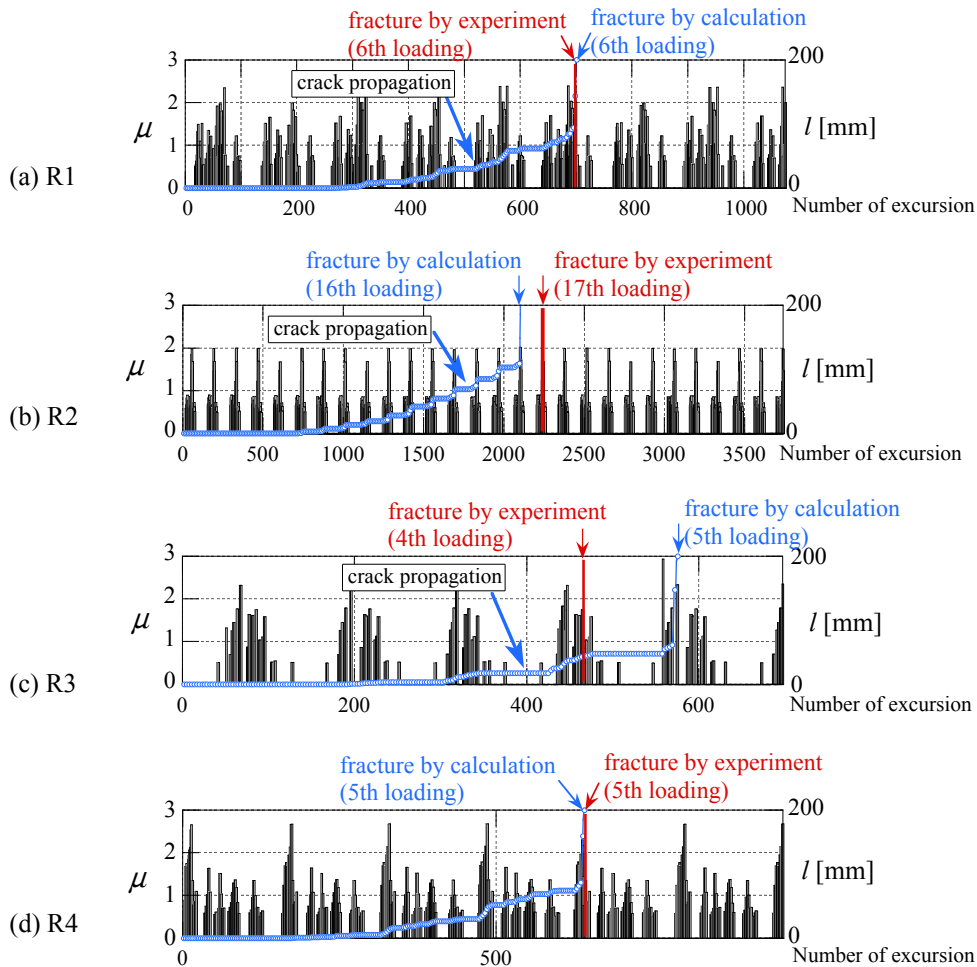


Figure 5.9 Damage evaluation by crack propagation ($\mu_0=0.5$)

6. CONCLUSIONS

In order to evaluate deformation capacity and predict fracture of welded moment connections subjected to cyclic plastic deformations, a series of cyclic loading tests were conducted and the following results were obtained.

- 1) A series of constant amplitude cyclic loading tests were conducted and the relationships between number of cycles at fracture and ductility amplitude were obtained. Based on observation of crack propagation along weld lines, a method to evaluate crack propagation considering effect of ductility amplitude is proposed.
- 2) A series of two-stage constant amplitude cyclic loading tests were conducted and the effect of variable amplitudes on deformation capacity is observed. The order of different amplitudes effects on damage index and the damage index by two-stage constant amplitude tests are evaluated by proposed

evaluation method using crack propagation formulation.

3) A series of random amplitude cyclic loading tests simulating response of highrise buildings by long-period earthquakes were conducted. The damage index and the fracture of welded connection are evaluated by using proposed crack propagation formulation, the instance of fracture is well predicted by taking into account effects of loadings by small amplitude whose ductility is larger than 0.5.

ACKNOWLEDGEMENT

This research was supported by the Grants-in-Aid for Scientific Research (A), KAKENHI (No.21246087), from Japan Society for the Promotion of Science (JSPS).

REFERENCES

- ASTM Standard E1049-85 (2005). Standard practices for cycle counting in fatigue analysis. ASTM International.
- Campbell, S.D., Richard, R.M. and Partridge, J.E. (2008) Steel moment damage prediction using low-cycle fatigue. *Proceedings of the 14th WCEE*, 0255.
- Iyama, I. and Ricles, J.M. (2009). Prediction of Fatigue Life of Welded Beam-to-Column Connections under Earthquake Loading. *Journal of Structural Engineering*, 135:12, ASCE. 1472-1480.
- JASS 6 steel work (2007). Japanese architectural standard specification, Architecture Institute of Japan, (in Japanese).
- Kadono, D., Jiao, Y., Shimada, Y., Kishiki, S. and Yamada S. (2008). Study on energy dissipation capacity of beam under random cyclic loading, Architectural Institute of Japan, *Summaries of technical papers of annual meeting, Structures III*, 567-570. (in Japanese)
- Kamae, K., Kawabe, H., Irikura, K. (2004). Strong Ground Motion Prediction for Huge Subduction Earthquakes using a Characterized Source Model and Several Simulation Techniques, *Proceedings of 13th WCEE*, 655.
- Kasai, K., Pu, W.C. and Wada, A. (2012). Responses of tall buildings in Tokyo during the 2011 Great East Japan Earthquake, *Proceedings of the 7th International Conference on Behavior of Steel Structures in Seismic Areas, STESSA 2012*. 25-35.
- Kuwamura, H. and Takagi, N. (2004). Similitude law of prefracture hysteresis of steel members. ASCE, *Journal of Structural Engineering* **130:5**, 752-761.
- Miner, M.A. (1945). Cumulative damage in fatigue. *Trans. ASME, Journal of Applied Mechanics*, 67, 159-164.
- Stojadinovic, B. (2003). Stability and low-cycle fatigue limits of moment connection rotation capacity. *Engineering Structures* **25:5**, 691-700.
- Suita, K. (2012). Seismic evaluation and retrofit of welded moment connection of early high-rise buildings subjected to long-period ground motions. *Proceedings of the Seventh International Conference on Behavior of Steel Structures in Seismic Areas, STESSA 2012*. 1057-1063.
- Suzuki, W., Iwata, T., Asano, K. & Yamada, N. (2005). Estimation of the source model for the foreshock of the 2004 off the Kii Peninsula earthquakes and strong ground motion simulation of the hypothetical Tonankai earthquake using the empirical Green's function method, *Earth Planets Space*, **57**, 345-350.
- Tsuruki, M., Zhao, B.M., Anatoly, P. & Kagawa, T. (2005). Strong ground motion prediction in Osaka prefecture during the Nankai and Tonankai Earthquake: Japan Society of Civil Engineers, *Journal of Structural Engineering*, **51A**, 501-502.
- Zhou, Z., Ito, T. and Kuwamura, H. (2008). Geometrical and Metallurgical Notches of Welded Joints of steel beam-to-column connections, Part 5. Tests of equivalent notches specimens under variable amplitude loadings, Architectural Institute of Japan, *Summaries of technical papers of annual meeting, Structures III*, 999-1000. (in Japanese)